

Received April 26, 2019, accepted May 15, 2019, date of publication May 20, 2019, date of current version June 13, 2019.

Digital Object Identifier 10.1109/ACCESS.2019.2917705

# Dissolved Gas Analysis in Transformer Oil Using Pt-Doped WSe<sub>2</sub> Monolayer Based on First Principles Method

ZHENWEI CHEN<sup>1</sup>, XIAOXING ZHANG<sup>1,2</sup>, HAO XIONG<sup>3</sup>, DACHANG CHEN<sup>1</sup>,  
HONGTU CHENG<sup>1</sup>, JU TANG<sup>1,4</sup>, YUAN TIAN<sup>1</sup>, AND SONG XIAO<sup>1</sup>

<sup>1</sup>School of Electrical Engineering and Automation, Wuhan University, Wuhan 430072, China

<sup>2</sup>School of Electrical and Electronic Engineering, Hubei University of Technology, Wuhan 430068, China

<sup>3</sup>Maintenance Branch Company, State Grid Chongqing Electric Power Company, Chongqing 400039, China

<sup>4</sup>State Key Laboratory of Power Transmission Equipment and System Security and New Technology, Chongqing University, Chongqing 400044, China

Corresponding author : Xiaoxing Zhang (xiaoxing.zhang@outlook.com) and Song Xiao (xiaosong@whu.edu.cn)

**ABSTRACT** The composition and content of dissolved gases in transformer oil are closely related to the type of faults in the transformer and the severity of potential hazards. Dissolved gas analysis (DGA) in insulating oil is an important way to monitor the state of transformer equipment. CO, CH<sub>4</sub>, and C<sub>2</sub>H<sub>2</sub> are one of the dissolved gases in the transformer oil. Based on the density functional theory, the optimal adsorption site of the transition metal atom Pt on the surface of WSe<sub>2</sub>, one of the typical layered transition metal disulfides (LTMDs), is determined in the beginning. Attaining the adsorption behavior of these three gases on the surface of Pt-WSe<sub>2</sub>. The optimal structure of gas adsorption, charge transfer, adsorption energy, electronic density of states (DOS), deformation charge density (DCD), and frontier orbital are analyzed. As an electron acceptor, Pt-WSe<sub>2</sub> attracts electrons from all three gas molecules. The adsorption type of CO and C<sub>2</sub>H<sub>2</sub> molecules is chemisorption, whose adsorption effect is strong. The CH<sub>4</sub> adsorption is physical adsorption, whose adsorption effect is weak. The adsorption of all the three gas molecules leads to an increase in the bandgap of the Pt-WSe<sub>2</sub>, that is, the increase in the resistivity.

**INDEX TERMS** Adsorption, transformer oil, Pt-WSe<sub>2</sub> monolayer, DGA, first-principles calculation.

## I. INTRODUCTION

Layered transition metal disulfides (LTMDs) have received considerable attentions as one of the most two-dimensional (2D) materials recently, and LTMDs have overcome the shortcomings of the zero band gap exists in another two-dimensional carbon-based nanomaterial graphene [1], [2], greatly expanding the sensing applications of these new materials, which exhibit strong anisotropy in mechanics, electricity, thermodynamics, etc. For example, both WSe<sub>2</sub> and MoS<sub>2</sub> show obvious features, such as indirect-direct Band gap crossing, topological superconductivity, interlayer tunable band gap and selective photoexcitation [3]–[5]. The unique properties of LTMDs make it a promising application in fields of field effect transistors, flexible electronics, optoelectronics, electronics, electrocatalysts and photocatalysts [6]–[9]. This work focuses on the large surface/volume ratios, high

electron activity and sensitivity of layered two-dimensional materials [10]–[16], which may therefore be potential for sensor applications. In addition, recent reports have confirmed that transition metal (TM) doping LTMDs can greatly enhance their sensitive response to gas molecules, which can be attributed to strong orbits interaction between gas molecules and the doped TM atoms [17].

Oil-immersed power transformers account for more than 90% of all types of transformers, considered to be the most important and valuable equipment in power systems [18]. However, there exists very phenomenon in the long-running transformers, such as the overheating of insulation oil or isolating paper, partial discharge, arc discharge, spark discharge, water ingress and dampness, natural aging, etc. When those situations happen in the oil-immersed power transformer, the transformer oil suffers electricity and heat, which would produce low molecular hydrocarbons, i.e. Methane (CH<sub>4</sub>), ethane (C<sub>2</sub>H<sub>6</sub>), ethylene (C<sub>2</sub>H<sub>4</sub>), acetylene (C<sub>2</sub>H<sub>2</sub>), and H<sub>2</sub>, CO, CO<sub>2</sub> and other gases [19]–[21].

The associate editor coordinating the review of this manuscript and approving it for publication was Sanket Goel.

The composition and content of such mixed gas are closely related to the type of fault and severity of transformer failure, besides, to some extent the failure happened in the transformer means a serious electrical accident, such as a large-scale blackout. So monitoring the composition and content of gases dissolved in the oil is essential to ensure the stable operation of the power system and prevent damage to the national economy. Dissolved gas analysis (DGA) in transformer oil has become an important method for monitoring transformer equipment [22] and is widely considered as a feasible and important method for estimating the operating state of oil-filled power transformers by detecting typical dissolved gases. Currently, there are two major methods for gas detection, namely, electrical and optical methods [23]–[25], among which gas sensor belongs to the category of electrical detection methods. At present, there are continuous researches to propose the use of different materials and their modified or doped materials for making gas sensors for on-line monitoring of gas concentration and types [26]–[29], among which there are studying which concern about such application in online monitoring of dissolved gases in insulating oil [30]–[32], which is a forward-looking approach because of the advantages of simple structure, fast response, low cost, low power consumption and so on.

In this work, Pt-doped single-layer WSe<sub>2</sub> (Pt-WSe<sub>2</sub>) was proposed as a promising sensing material for detecting dissolved gases in transformer oil. At first, the possible stable structure of single-layer Pt-WSe<sub>2</sub> was studied. The stable structure with the lowest energy was selected to the adsorption study with three typical gases, including CO, CH<sub>4</sub> and C<sub>2</sub>H<sub>2</sub>. The geometric and electronic structures of the three adsorption systems were analyzed, which obtained the adsorption situation of molecules on the single layer of Pt-WSe<sub>2</sub>. In addition, the sensing principle of the material surface is described to provide evidence for its application as a potentially superior gas sensing material in DGA.

## II. COMPUTATIONAL METHOD

First-principles calculations have been performed in the framework of DFT using Dmol<sup>3</sup> package of materials studio [33], [34]. The unrestricted density functional theory plus dispersion (DFT-D) calculation were performed in this work [35], [36]. The exchange-correlation energy was calculated by the generalized approximation (GGA) method with the Perdew-Burke-Ernzerhof (PBE) function [37]–[40]. This method is widely utilized used in the calculation of materials and their surfaces with DFT calculation. This work applied The Tkatchenko and Scheffler's (TS) method to correct the Van der Waals' force for obtaining more accurate results [41], [42]. The DFT Semi-core Pseudopotentials (DSSP) and the double numerical atomic orbital augmented by d-polarization (DNP) were used. The energy convergence tolerance, the maximum force and the maximum displacement of geometry optimizations were  $1.0 \times 10^{-5}$  Ha, 0.002 Ha/Å and 0.005Å [43]. The global orbital cutoff radius was set at 5.0Å. The Brillouin zone is sampled using a  $8 \times 8 \times 1$

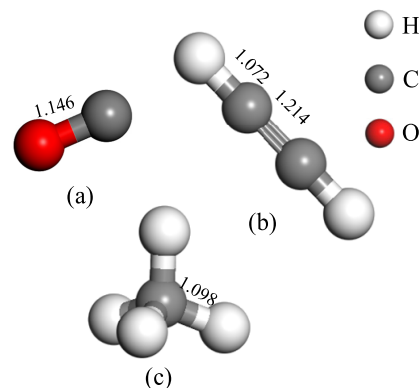


FIGURE 1. Structures of gases (a) CO; (b) C<sub>2</sub>H<sub>2</sub>; (c) CH<sub>4</sub>.

Monkhorst-Pack k-point grid for the calculation of densities of states (DOS), in the meantime, a  $3 \times 3 \times 1$  Monkhorst-Pack k-point grid for others.

We obtain an optimized lattice parameter of 3.282 Å which is consistency with other researches and experiment results in literature [3] and [5], which proves the accuracy of simulation parameter setting. A  $(4 \times 4)$  supercell including 16 W and 32 Se is built with a vacuum region of  $c = 15$  Å in order to avoid the interaction with adjacent layers.

The adsorption energy ( $E_{ad}$ ) of gas adsorption process were calculated by the following equation:

$$E_{ad} = E_{molecular/Pt-WSe_2} - E_{molecular} - E_{Pt-WSe_2} \quad (1)$$

where the  $E_{molecular/Pt-WSe_2}$ ,  $E_{molecular}$  and  $E_{Pt-WSe_2}$  denoted energy of the adsorption system, isolated Pt-WSe<sub>2</sub> and gas molecule, respectively.

In addition, the Mullikan population analysis were considered to analyze the charge transfer ( $Q_t$ ) between the gas molecule and the surface, characterized by deformation electron value by gas molecule after adsorption. In this work, If  $Q_t > 0$ , it means that electrons transfer from Pt-WSe<sub>2</sub> to gas molecule and when  $Q_t < 0$ , the electrons transfer from gas molecule to Pt-WSe<sub>2</sub>.

## III. RESULTS AND DISCUSSION

### A. GAS MOLECULAR AND Pt-WSe<sub>2</sub> STRUCTURE

Before the adsorption behavior study, the molecular structures of the gases (CO, CH<sub>4</sub>, C<sub>2</sub>H<sub>2</sub>) was geometrically optimized to obtain the most stable structure. The optimal gas structure is shown in Fig. 1. The geometric structure is consistent with the previous literatures [18], [22]. The C-O bond length of CO molecule is 1.146 Å, and the molecular structure of C<sub>2</sub>H<sub>2</sub> is linear, in which the C-C bond and C-H bond are 1.214 Å and 1.072 Å, respectively, while CH<sub>4</sub> is a regular octahedral structure with a C-H bond length of 1.098 Å. The carbon atom with sp hybridized orbital has stronger electronegativity than that of CH<sub>4</sub> with sp<sup>3</sup> hybridization, so the C-H bond of the C<sub>2</sub>H<sub>2</sub> molecule is shorter than CH<sub>4</sub>.

The Pt-WSe<sub>2</sub> monolayer was modeled as single Pt atom adsorption onto the intrinsic WSe<sub>2</sub> monolayer, where four

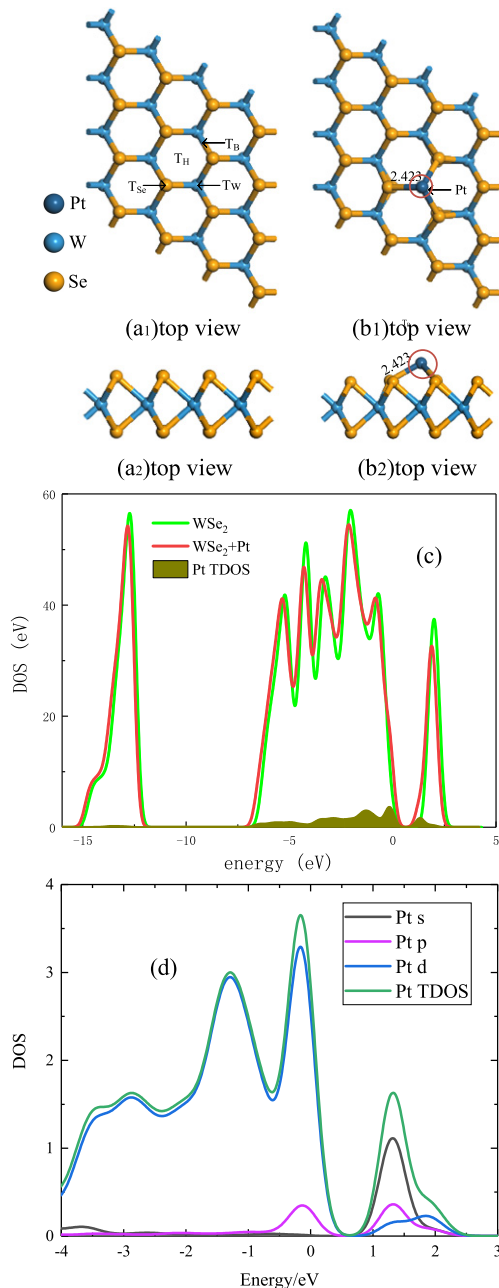


**FIGURE 2. Geometric structure and electronic behavior of WSe<sub>2</sub> with doping or not. (a) WSe<sub>2</sub>; (b) Pt-WSe<sub>2</sub>; (c) DOS; (d) DOS of Pt which doped into WSe<sub>2</sub>.**

possible sites were considered, marked as T<sub>H</sub> (above the center of the hexagonal ring of WSe<sub>2</sub>), T<sub>W</sub> (at the top of the W atom), T<sub>Se</sub> (at the top of Se atom) and T<sub>B</sub> (the bridge site between two Se atoms), respectively. The structural energy at different doping sites is obtained by geometric optimization. The lower the energy, the more stable the structure. By comparison, the T<sub>W</sub> doping method with the lowest energy was chosen to perform the following gases adsorption studies. The geometry and DOS diagram before and after doping are shown in Fig. 2. The distance between the Pt atom and the Se atom is 2.423 Å. After doping,

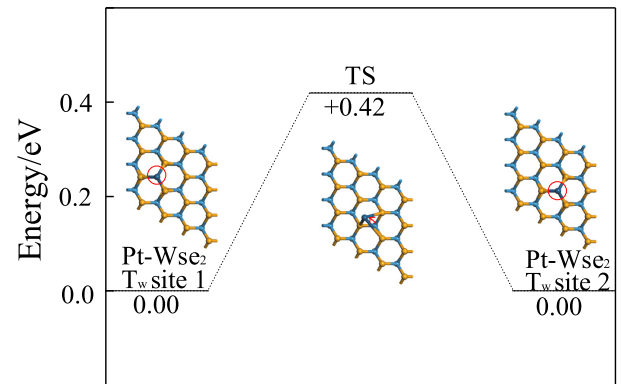


**FIGURE 3. Movement of Pt atom on WSe<sub>2</sub>.**

DOS appears to move left, resulting from the electrons of WSe<sub>2</sub> are attracted by Pt atoms, making the Fermi level shifting to the right. As shown, it can also be seen that the width of band gap is reduced after doping.

Since the band structure near the Fermi level determines the physical properties of the conductivity, only the DOS between -4eV and 3eV near the Fermi level is given in FIG. 2(d). The energy at the Fermi level is usually set to 0eV, and the other energies are taken as the relative values of the Fermi level. In combination with partial density of states (PDOS), it can be seen from the Fig 3(d) that the p and d orbital electron of Pt atoms make contribution to the conduction band and valence band of WSe<sub>2</sub> and Pt s orbital electronic contribute to the conduction band only, it is worth noting that in the position of about 1.3 eV, due to the contribution of Pt atom each orbital electron(s, p, d), it's resulting in that the gap between the conduction band and valence band gap decreases, seen in the position (about 1.3 eV) of Pt-WSe<sub>2</sub> DOS in figure 2(c).

In order to study the stability of the Pt atom on the surface of the two-dimensional WSe<sub>2</sub>, as shown in Fig. 3, the reaction energy barrier of the Pt metal atom moving from T<sub>W</sub> to another nearest T<sub>W</sub> is calculated, and the calculated energy barrier value is 0.42 eV. Because it is smaller than the critic barrier of Pt atom, 0.81eV [44], this study suggests that methods should be taken to prevent the agglomeration of Pt atoms on the surface of WSe<sub>2</sub> in the Pt-doped WSe<sub>2</sub> experiment [45], such as the method of freeze-drying and so on.

### B. ADSORPTION BEHAVIOUR ANALYSIS OF DISSOLVED GASES ON Pt-WSe<sub>2</sub> MONOLAYER

The lowest energy optimal adsorption is obtained by putting closely gas molecules to the surface of Pt-WSe<sub>2</sub> at different placement sites. Fig. 4 shows the most stable adsorption structure and corresponding deformation charge density (DCD) of the different gases (C<sub>2</sub>H<sub>2</sub>, CH<sub>4</sub>, CO) on Pt-WSe<sub>2</sub>, the information shown in TABLE 1 include the distance of different atoms, adsorption energy and charge transfer.

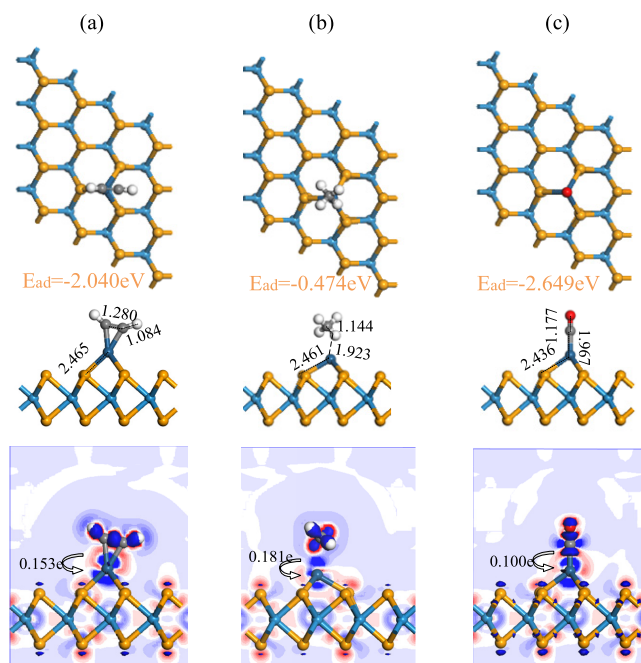


**FIGURE 4.** Adsorption configurations and DCD for different gas systems. (a)  $C_2H_2$  system. (b)  $CH_4$  system. (c)  $CO$  system. The figures from top to bottom are the top view, side view and DCD for gas adsorption for gas adsorption in sequence (The red and blues regions respect the electron accumulation and electron depletion respectively, with unit taken as  $e/\text{\AA}^3$ .)

**TABLE 1.** Parameters for gases adsorption system: Adsorption energy, total charge transfer, distance.

Configuration	$E_{ad}(eV)$	$Q_{t-Mulliken}$	Distance( $\text{\AA}$ )
$C_2H_2$ system	-2.040	-0.153	C-Pt:1.084
$CH_4$ system	-0.474	-0.181	H-Pt:1.923
$CO$ system	-2.649	-0.100	C-Pt:1.967

The most stable adsorption structure of  $C_2H_2$  system and its DCD are shown in Fig. 4(a). The C atom of  $C_2H_2$  molecule is strongly attracted by Pt atoms. The distance between Pt-C is only 1.084  $\text{\AA}$ , which is smaller than the distance 1.280  $\text{\AA}$  of C-C bond in gas molecules. The reaction between gas molecule with Pt-WSe<sub>2</sub> is strong. The molecular structure of  $C_2H_2$  is severely deformed due to the adsorption effect from the Pt-WSe<sub>2</sub>. The molecular structure no longer appears linear and bends, and the C-C bond is stretched from 1.214  $\text{\AA}$  to 1.280  $\text{\AA}$ , an increase of 0.076  $\text{\AA}$ . There is also a tensile phenomenon in the C-H bond, which indicates that the  $C_2H_2$  molecule is activated. It can be known from the calculation of the adsorption energy that the adsorption energy is as high as  $-2.040\text{eV}$  (the negative sign indicates that the adsorption process is an exothermic process), and it is proved that the adsorption is very strong and belongs to chemical adsorption. Through Mulliken charge analysis and DCD analysis, it was found that  $C_2H_2$  transferred 0.153e electrons to the surface of the 2D material. The gas molecule acts as electron donor, and the transferred electrons mostly surround the Pt atoms,

reflecting the common characteristics of transition metals: strong electron acceptor property. All the above phenomena indicate that  $C_2H_2$  gas molecule have a strong adsorption on the surface.

In terms of  $CH_4$  adsorption system, the optimal adsorption structure and the corresponding DCD are shown in Fig. 4(b), the  $CH_4$  gas molecule tends to approach Pt-WSe<sub>2</sub> through the H atom, and the shortest adsorption distance between them is 1.923  $\text{\AA}$ , and the corresponding adsorption energy is  $-0.474\text{eV}$ . The C-H bond in the gas molecule is slightly stretched, extending from 1.098  $\text{\AA}$  to 1.144  $\text{\AA}$ . The adsorption of  $CH_4$  system is not strong than  $C_2H_2$ 's, which belongs to the range of physical adsorption. According to the Mulliken analysis,  $CH_4$  loses 0.181e electrons, and the gas acts as an electron donor, which is the same as the  $C_2H_2$  analyzed in the upper part.

Similarly, Fig. 4(c) shows the optimal adsorption structure and corresponding DCD for the CO adsorption system. CO is trapped by the metal atom Pt through the C atom, and the distance of C-Pt is 1.967  $\text{\AA}$ . In the adsorption system, the C-O molecule is stretched, the C-O bond is extended from 1.146  $\text{\AA}$  to 1.177  $\text{\AA}$ , and the adsorption energy is as high as  $-2.649\text{eV}$ . A strong chemical reaction occurs between CO and Pt-WSe<sub>2</sub>, in the meantime, CO transfers 0.100e electrons to Pt-WSe<sub>2</sub>.

### C. DOS ANALYSIS OF DISSOLVED GASES ON Pt-WSe<sub>2</sub> MONOLAYER

To further explore the interaction mechanism between gas molecules and surface, Fig. 5 shows the density of states including the electron orbitals of each atom.

The DOS of the Pt-WSe<sub>2</sub>/ $C_2H_2$  system is shown in Fig. 5(a), the electron behavior in the adsorption reaction can be obtained by comparison with Pt-WSe<sub>2</sub> before and after adsorption. As shown in Fig. 5 (a1), the electron density TDOS after adsorption increased at  $-15\text{eV}$ ,  $-4\text{eV}$ , and a new peak appeared near  $-9\text{eV}$ ,  $-8\text{eV}$ , compared to Pt-WSe<sub>2</sub> before adsorption. This is due to the adsorption of  $C_2H_2$ . From Figure 5 (a3), it can be clearly seen that the DOS of the  $C_2H_2$  molecule before and after adsorption, the gas molecule DOS moves to the left after adsorption, and the peaks appearing at  $15\text{eV}$ ,  $-9\text{eV}$ ,  $-8\text{eV}$ , and  $-4\text{eV}$  of adsorbed  $C_2H_2$  molecule in Fig. 5 (a3) correspond exactly to that in Fig. 5(a1), which means  $C_2H_2$  has a strong adsorption effect on the surface of the material. The DOS of  $C_2H_2$  decreased after adsorption, which was caused by the loss of electrons in gas molecules, consistent with the before mentioned Mulliken analysis results. In Fig. 5 (a1), DOS is slightly shifted to the right after adsorption, combined with the electron transfer direction, it is determined that this is due to fact that the adsorbed gas molecule transfers electrons to the material, and thus the Fermi level shifts to the left. From Fig. 5 (a2), it can be observed that the peaks of Pt 4d and C 2p in the system show significant overlap around  $-15\text{eV}$ ,  $-9\text{eV}$ ,  $-8\text{eV}$ ,  $-1\text{eV}$ ,  $0\text{eV}$  and  $2\text{eV}$ , where exists serious orbital hybridization, indicating electron orbit interaction between



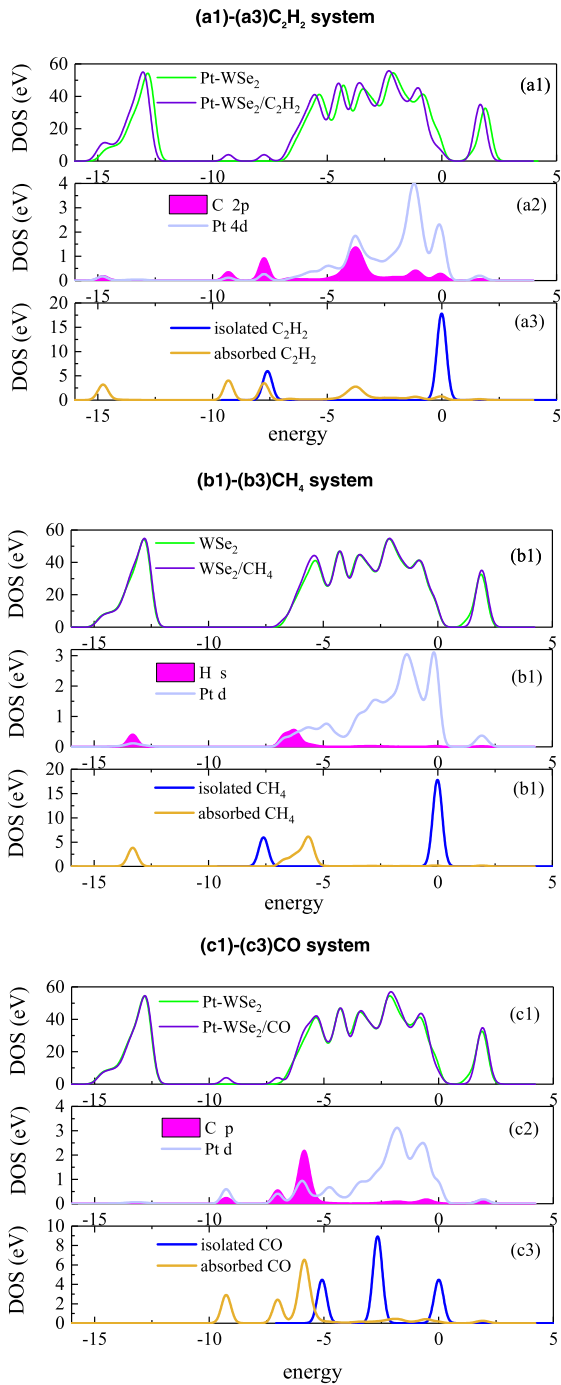


FIGURE 5. DOS distribution of different gas adsorption systems.

Pt and C<sub>2</sub>H<sub>2</sub> is very strong, and it is exactly the orbital hybridization of C atom and Pt atom that causes the movement of the peak position of the electronic density of state in Fig. (a2), showing the left shift of C<sub>2</sub>H<sub>2</sub> after adsorption.

Fig. 5(b) shows the DOS of the Pt-WSe<sub>2</sub>/CH<sub>4</sub> system, and Fig. 5(b1) shows the total density of states (TDOS) of the Pt-WSe<sub>2</sub> with adsorption or not. There are no obvious changes, only certain degrees of overlap at -13eV, -6eV. The 1s orbital electrons of the H atom captured by Pt-WSe<sub>2</sub>

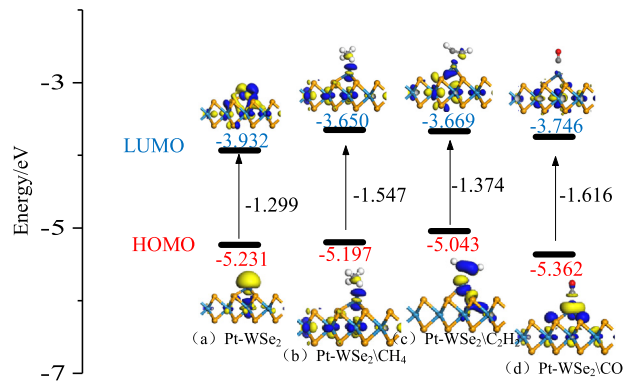


FIGURE 6. HOMO & LUMO distribution and related  $E_g$  for system before and after gas absorption. (a) Pt-WSe<sub>2</sub> monolayer. (b) CH<sub>4</sub> system. (c) C<sub>2</sub> H<sub>2</sub> system. (d) CO system.

only appear somewhat obvious hybridization with the 4d orbital electrons of the Pt atom at the level of about -16eV. These phenomena indicate that the adsorption strength is a little weak.

Similarly, Fig. 5(c) shows the DOS of the Pt-WSe<sub>2</sub>/CO system, as shown in Fig. 5 (c1). Although the overall TDOS does not change a lot, it doesn't draw the conclusion that the adsorption is not strong. It can be seen from Fig. 5 (c3) that the DOS distribution of CO gas molecules after adsorption is between -10eV and -6eV, and in the same interval of 5(c1), two new peaks appear in TDOS, what's more, significant orbital hybridization occurred between C 2p electrons and Pt 4d electrons at -9eV, -7eV and -6eV energy level, indicating the strong adsorption between the CO and Pt-WSe<sub>2</sub>.

#### D. SENSING BEHAVIOR PREDICTION OF Pt-WSe<sub>2</sub> MONOLAYER FOR DGA

In the electronic mechanism, Pt as a dopant changes the electrostatic potential of the surface of the WSe<sub>2</sub> due to different electron affinities, resulting in a change of the surface barrier height, that is, the change occurs in the corresponding semiconductor resistance value. The gas molecules are captured by the surface through the Pt atom. Besides, the Pd atom acts as a catalyst to enhance the adsorption of the gas molecules and accelerate the electron exchange between the sensor and the test gas [46]. Resistive gas sensors detect gas by detecting changes in the resistance of gas sensitive materials before and after adsorption with different gas molecules. Based on the frontier orbital theory, it could directly react to the cause of change in conductivity. As shown in Fig. 6, the figure shows the HOMO and LUMO before and after adsorption. Before the gas molecules are adsorbed on Pt-WSe<sub>2</sub> surface, the HOMO and LUMO mainly distribute on the side of the Pt doping site, and the band gap width between HOMO and LUMO is 1.299 eV. As shown in Fig. 6(b)-(d), when the adsorbed gas molecules interact with the surface of Pt-WSe<sub>2</sub>, the orbital distribution of HOMO and LUMO is significantly extended to the gas molecules, and the molecular adsorption makes the band gap of the system varying in

different degrees. All the three change is the increasing in the width of the band gap. The influence of the three gases on the change of Pt-WSe<sub>2</sub> band gap after adsorption is as follows: CO > CH<sub>4</sub> > C<sub>2</sub>H<sub>2</sub>.

It is known that the relationship between resistivity and band gap can be determined by the following formula [47], [48]:

$$\sigma \propto e^{(-E_g/2k_B T)} \quad (2)$$

where  $\sigma$  (Siemens (S)), T (Kelvin (K)) indicate the conductivity of the sensing material and the test temperature, and  $k_B$  is the Boltzmann constant.

According to the molecular orbital theory, the increase of the band gap value means that the charge transfer in the system is more difficult, that is, when the temperature is constant, the conductivity is inversely proportional to the width of band gap, and the wider the band gap, the more difficult it is for the electron to be excited from the valence band to the conduction band, which's external performance is the increase in resistance. Therefore, we believe that all three gases adsorption will lead to the increase in the system resistivity. The gas molecule reacts with the surface of the 2D material, and there is electron transfer between them changing the band gap width of the material. The Pt doped WSe<sub>2</sub> electron holes concentration is much higher than the free electron concentration, which belongs to the p-type semiconductor. As the reducing gas (CO, CH<sub>4</sub> and C<sub>2</sub>H<sub>2</sub>) adsorbing on the p-type semiconductor, the gas transfers electrons to the semiconductor, which makes the number of holes in the semiconductor decreases, that is, the decrease of carriers leads to the increase of resistance. It needed to be noted that theoretical calculation of the frontier orbit can only be carried out when the k value is set to  $1 \times 1 \times 1$ . The accuracy of this setting is insufficient, but even so, combine with the forbidden band width marked in FIG. 6, which is obtained when the k value is set to  $8 \times 8 \times 1$ , the result can still provide guidance qualitatively the change trend of resistivity before and after adsorption.

In order to better understand the sensing performance of Pt-WSe<sub>2</sub>, we need to discuss the diffusion behavior of gases on the material. The study placed different gases on different sites ( $T_w$ ,  $T_{Se}$  and  $T_{Hollow}$ ) on the material surface for DFT calculation. However, the results showed that when the gas molecules are placed on the site ( $T_w$ ,  $T_{Se}$  and  $T_{Hollow}$ ) which is near Pt atoms, the molecules would move to the top of Pt and be captured by Pt within the simulation. This is because the activity of Pt is strong than others. Basing on that, we thought gas diffusion behavior on surface can be ignored. To verify the above conclusion further, the adsorption energy of the three gas molecules on the different sites of pure WSe<sub>2</sub> was given, seen in table 2.

The adsorption of gas adsorption on intrinsic selenide tungsten surface shown in table 2 is much lower than that on Pt-WSe<sub>2</sub>, concluding that gas molecules will not spread in the Pt-WSe<sub>2</sub> surface, but will firmly adsorbed onto the Pt atoms. Moreover, the adsorption energy is the energy

**TABLE 2. Adsorption energy for gases adsorbing on intrinsic Selenide tungsten under different site.**

Site	$T_{Se}$	$T_w$	$T_{Hollow}$
C <sub>2</sub> H <sub>2</sub>	-0.235eV	-0.238eV	-0.228eV
CH <sub>4</sub>	-0.185 eV	-0.187 eV	-0.151 eV
CO	-0.149 eV	-0.137 eV	-0.124 eV

required for desorption, and the big adsorption energy of the gas on Pt-WSe<sub>2</sub> also ensures that the gas will be difficult to diffuse.

#### IV. CONCLUSIONS

In this work, based on the first principle, the adsorption performance of transformer oil decomposition gas (CO, CH<sub>4</sub> and C<sub>2</sub>H<sub>2</sub>) on Pt-WSe<sub>2</sub> was theoretically studied in the Dmol<sup>3</sup> framework by material studio. The typical dimensionally layered transition metal sulfide, WSe<sub>2</sub> with Pt atom doping, was predicted to have the potential to act as a gas-sensitive material inside the insulating device in the electric power field. The electronic behavior of Pt-WSe<sub>2</sub> before and after adsorption was determined by DOS analysis and Mulliken analysis. The conductivity of the Pt-WSe<sub>2</sub> before and after adsorption was obtained by frontier orbital analysis. The adsorption behaviors and response mechanisms of the three gases were analyzed. The main conclusions were as follows: In term of the doping site of Pt metal atom on WSe<sub>2</sub>, Pt atom is more likely to be doping at the top of W atom, which marked as  $T_w$  in the paper. In practice experiment, methods are needed to adopt for preventing Pt Clusters formed on the surface of WSe<sub>2</sub>. The adsorption degrees between CO, CH<sub>4</sub>, C<sub>2</sub>H<sub>2</sub> gas and Pt-WSe<sub>2</sub> are different. CO and C<sub>2</sub>H<sub>2</sub> strongly adsorbed on the Pt doped WSe<sub>2</sub>, while the adsorption of CH<sub>4</sub> is weak. The former two are chemical adsorption, while the latter is physical adsorption. During the adsorption process, all three gases transfer electrons to Pt-WSe<sub>2</sub>, and the three adsorptions will lead to an increase in the width of band gap of the doping material, that is, the increase in resistivity. The corresponding resistivity of the three adsorption systems is: CO > CH<sub>4</sub> > C<sub>2</sub>H<sub>2</sub>.

#### REFERENCES

- [1] M. Ali and N. Tit, "Adsorption of NO and NO<sub>2</sub> molecules on defected-graphene and ozone-treated graphene: First-principles analysis," *Surf. Sci.*, vol. 684, pp. 28–36, Jun. 2019.
- [2] Y. Guo, Z. Chen, W. Wu, Y. Liu, and Z. Zhou, "Adsorption of NO<sub>x</sub> (x=1,2) gas molecule on pristine and B atom embedded  $\gamma$ -graphyne based on first-principles study," *Appl. Surf. Sci.*, vol. 455, pp. 484–491, Oct. 2018.
- [3] A. Kumar and P. K. Ahluwalia, "Electronic structure of transition metal dichalcogenides monolayers 1H-MX<sub>2</sub> (M = Mo, W; X=S,Se,Te) from ab-initio theory: New direct band gap semiconductors," *Eur. Phys. J. B*, vol. 85, p. 186, Jun. 2012.
- [4] K. F. Mak, C. Lee, J. Hone, J. Shan, and T. F. Heinz, "Atomically thin MoS<sub>2</sub>: A new direct-gap semiconductor," *Phys. Rev. Lett.*, vol. 105, Sep. 2010, Art. no. 136805.
- [5] D. Ma et al., "Interaction between H<sub>2</sub>O, N<sub>2</sub>, CO, NO, NO<sub>2</sub> and N<sub>2</sub>O molecules and a defective WSe<sub>2</sub> monolayer," *Phys. Chem. Chem. Phys.*, vol. 19, no. 38, pp. 26022–26033, 2017.
- [6] H. Sahin et al., "Anomalous Raman spectra and thickness-dependent electronic properties of WSe<sub>2</sub>," *Phys. Rev. B, Condens. Matter*, vol. 87, Apr. 2013, Art. no. 165409.

- [7] J. S. Ross *et al.*, "Electrically tunable excitonic light-emitting diodes based on monolayer WSe<sub>2</sub> p-n junctions," *Nature Nanotechnol.*, vol. 9, pp. 268–272, Mar. 2014.
- [8] A. Abbasi and J. J. Sardroodi, "Adsorption of O<sub>3</sub>, SO<sub>2</sub> and SO<sub>3</sub> gas molecules on MoS<sub>2</sub> monolayers: A computational investigation," *Appl. Surf. Sci.*, vol. 469, pp. 781–791, Mar. 2019.
- [9] A. Abbasi and J. J. Sardroodi, "Prediction of a highly sensitive molecule sensor for SO<sub>x</sub> detection based on TiO<sub>2</sub>/MoS<sub>2</sub> nanocomposites: A DFT study," *J. Sulfur Chem.*, vol. 38, pp. 52–68, Oct. 2016.
- [10] V. Kumar and D. R. Roy, "Single-layer stanane as potential gas sensor for NO<sub>2</sub>, SO<sub>2</sub>, CO<sub>2</sub> and NH<sub>3</sub> under DFT investigation," *Phys. E, Low-Dimensional Syst. Nanostruct.*, vol. 110, pp. 100–106, Jun. 2019.
- [11] D. Yang, X. Fan, D. Zhao, Y. An, Y. Hu, and Z. Luo, "Sc<sub>2</sub>CO<sub>2</sub> and Mn-doped Sc<sub>2</sub>CO<sub>2</sub> as gas sensor materials to NO and CO: A first-principles study," *Phys. E, Low-Dimensional Syst. Nanostruct.*, vol. 111, pp. 84–90, Jul. 2019.
- [12] G. Zhao and M. Li, "Ni-doped MoS<sub>2</sub> biosensor: A promising candidate for early diagnosis of lung cancer by exhaled breathe analysis," *Appl. Phys. A*, vol. 124, p. 751, Nov. 2018.
- [13] D. Zhang, C. Jiang, P. Li, and Y. E. Sun, "Layer-by-layer self-assembly of Co<sub>3</sub>O<sub>4</sub> nanorod-decorated MoS<sub>2</sub> nanosheet-based nanocomposite toward high-performance ammonia detection," *ACS Appl. Mater. Interfaces*, vol. 9, pp. 6462–6471, Jan. 2017.
- [14] M. Chhowalla, H. S. Shin, G. Eda, L.-J. Li, K. P. Loh, and H. Zhang, "The chemistry of two-dimensional layered transition metal dichalcogenide nanosheets," *Nature Chem.*, vol. 5, no. 4, pp. 263–275, 2013.
- [15] A. Abbasi and J. J. Sardroodi, "The adsorption of sulfur trioxide and ozone molecules on stanene nanosheets investigated by DFT: Applications to gas sensor devices," *Phys. E, Low-Dimensional Syst. Nanostruct.*, vol. 108, pp. 382–390, Apr. 2019.
- [16] A. Abbasi, "Theoretical investigation of the interaction between noble metals (Ag, Au, Pd, Pt) and stanene nanosheets: A DFT study," *J. Inorganic Organometallic Polym. Mater.*, Apr. 2019. doi: 10.1007/s10904-019-01151-x.
- [17] D. Chen, X. Zhang, J. Tang, J. Fang, Y. Li, and H. Liu, "Adsorption and dissociation mechanism of SO<sub>2</sub> and H<sub>2</sub>S on Pt decorated graphene: A DFT-D<sub>3</sub> study," *Appl. Phys. A*, vol. 124, p. 404, Jun. 2018.
- [18] H. Cui, X. Zhang, G. Zhang, and J. Tang, "Pd-doped MoS<sub>2</sub> monolayer: A promising candidate for DGA in transformer oil based on DFT method," *Appl. Surf. Sci.*, vol. 470, pp. 1035–1042, Mar. 2019.
- [19] J. Ding *et al.*, "New sensor for gases dissolved in transformer oil based on solid oxide fuel cell," *Sens. Actuators B, Chem.*, vol. 202, pp. 232–239, Oct. 2014.
- [20] T. Mak *et al.*, "Optical fiber sensor for the continuous monitoring of hydrogen in oil," *Sens. Actuators B, Chem.*, vol. 190, pp. 982–989, Jan. 2014.
- [21] Q. Zhang, Q. Zhou, Z. Lu, Z. Wei, L. Xu, and Y. Gui, "Recent advances of SnO<sub>2</sub>-based sensors for detecting fault characteristic gases extracted from power transformer oil," *Frontiers Chem.*, vol. 6, p. 364, Aug. 2018.
- [22] H. Cui, D. Chen, Y. Zhang, and X. Zhang, "Dissolved gas analysis in transformer oil using Pd catalyst decorated MoSe<sub>2</sub> monolayer: A first-principles theory," *Sustain. Mater. Technol.*, vol. 20, Jul. 2019, Art. no. e00094.
- [23] G. Modugno, C. Corsi, M. Gabrysch, and M. Inguscio, "Detection of H<sub>2</sub>S at the ppm level using a telecommunication diode laser," *Opt. Commun.*, vol. 145, nos. 1–6, pp. 76–80, 1998.
- [24] K. Chen, B. Zhang, S. Liu, and Q. Yu, "Parts-per-billion-level detection of hydrogen sulfide based on near-infrared all-optical photoacoustic spectroscopy," *Sens. Actuators B, Chem.*, vol. 283, pp. 1–5, Mar. 2019.
- [25] X. Yin *et al.*, "Ppb-level photoacoustic sensor system for saturation-free CO detection of SF<sub>6</sub> decomposition by use of a 10 W fiber-amplified near-infrared diode laser," *Sens. Actuators B, Chem.*, vol. 282, pp. 567–573, Mar. 2019.
- [26] Q. Zhou *et al.*, "Fabrication and characterization of highly sensitive and selective sensors based on porous NiO nanodisks," *Sens. Actuators B, Chem.*, vol. 259, pp. 604–615, Apr. 2018.
- [27] D. Zhang, Y. Sun, P. Li, and Y. Zhang, "Facile fabrication of MoS<sub>2</sub>-modified SnO<sub>2</sub> hybrid nanocomposite for ultrasensitive humidity sensing," *ACS Appl. Mater. Interfaces*, vol. 8, no. 22, pp. 14142–14149, 2016.
- [28] Q. Zhou *et al.*, "Highly sensitive carbon monoxide (CO) gas sensors based on Ni and Zn doped SnO<sub>2</sub> nanomaterials," *Ceramics Int.*, vol. 44, pp. 4392–4399, Mar. 2018.
- [29] A. Yang, D. Wang, X. Wang, D. Zhang, N. Koratkar, and M. Rong, "Recent advances in phosphorene as a sensing material," *Nano Today*, vol. 20, pp. 13–32, Jun. 2018.
- [30] A. I. Uddin, U. Yaqoob, and G.-S. Chung, "Dissolved hydrogen gas analysis in transformer oil using Pd catalyst decorated on ZnO nanorod array," *Sens. Actuators B, Chem.*, vol. 226, pp. 90–95, Jan. 2016.
- [31] M. R. Samsudin, Y. G. Shee, F. R. M. Adikan, B. B. A. Razak, and M. Dahari, "Fiber Bragg gratings hydrogen sensor for monitoring the degradation of transformer oil," *IEEE Sensors J.*, vol. 16, no. 9, pp. 2993–2999, May 2016.
- [32] J. Bodzenta, B. Burak, Z. Gacek, W. P. Jakubik, S. Kochowski, and M. Urbańczyk, "Thin palladium film as a sensor of hydrogen gas dissolved in transformer oil," *Sens. Actuators B, Chem.*, vol. 87, no. 1, pp. 82–87, 2002.
- [33] Q. Wan, Y. Xu, and H. Xiao, "Exhaled gas detection by Ir-doped CNT for primary diagnosis of lung cancer," *AIP Adv.*, vol. 8, Oct. 2018, Art. no. 105128.
- [34] D. Zhao, X. Fan, Z. Luo, Y. An, and Y. Hu, "Enhanced gas-sensing performance of graphene by doping transition metal atoms: A first-principles study," *Phys. Lett. A*, vol. 382, pp. 2965–2973, Oct. 2018.
- [35] X. Zhang, Z. Chen, D. Chen, H. Cui, and J. Tang, "Adsorption behaviour of SO<sub>2</sub> and SOF<sub>2</sub> gas on Rh-doped BNNT: A DFT study," *Mol. Phys.*, Mar. 2019. doi: 10.1080/00268976.2019.1580394.
- [36] Q. Wan, Y. Xu, X. Chen, and H. Xiao, "Exhaled gas detection by a novel Rh-doped CNT biosensor for prediagnosis of lung cancer: A DFT study," *Mol. Phys.*, vol. 116, pp. 2205–2212, May 2018.
- [37] D. Liu *et al.*, "Adsorption of SF<sub>6</sub> decomposition components over Pd (111): A density functional theory study," *Appl. Surf. Sci.*, vol. 465, pp. 172–179, Jan. 2019.
- [38] D.-W. Wang *et al.*, "MoTe<sub>2</sub>: A promising candidate for SF<sub>6</sub> decomposition gas sensors with high sensitivity and selectivity," *IEEE Electron Device Lett.*, vol. 39, no. 2, pp. 292–295, Feb. 2018.
- [39] X. H. Wang *et al.*, "Effects of adatom and gas molecule adsorption on the physical properties of tellurene: A first principles investigation," *Phys. Chem. Chem. Phys.*, vol. 20, no. 6, pp. 4058–4066, 2018.
- [40] A. Abbasi, "Adsorption of phenol, hydrazine and thiophene on stanene monolayers: A computational investigation," *Synth. Met.*, vol. 247, pp. 26–36, Jan. 2019.
- [41] D. Chen, X. Zhang, J. Tang, H. Cui, and Y. Li, "Noble metal (Pt or Au)-doped monolayer MoS<sub>2</sub> as a promising adsorbent and gas-sensing material to SO<sub>2</sub>, SOF<sub>2</sub> and SO<sub>2</sub>F<sub>2</sub>: A DFT study," *Appl. Phys. A*, vol. 124, p. 194, Feb. 2018.
- [42] Y. Li, X. Zhang, D. Chen, S. Xiao, and J. Tang, "Adsorption behavior of COF<sub>2</sub> and CF<sub>4</sub> gas on the MoS<sub>2</sub> monolayer doped with Ni: A first-principles study," *Appl. Surf. Sci.*, vol. 443, pp. 274–279, Jun. 2018.
- [43] D. Zhang, J. Wu, P. Li, and Y. Cao, "Room-temperature SO<sub>2</sub> gas-sensing properties based on a metal-doped MoS<sub>2</sub> nanoflower: An experimental and density functional theory investigation," *J. Mater. Chem. A*, vol. 5, no. 39, pp. 20666–20677, 2017.
- [44] Q. G. Jiang, Z. M. Ao, S. Li, and Z. Wen, "Density functional theory calculations on the CO catalytic oxidation on Al-embedded graphene," *RSC Adv.*, vol. 4, pp. 20290–20296, Apr. 2014.
- [45] P. Wu, N. Yin, P. Li, W. Chenga, and M. Huang, "The adsorption and diffusion behavior of noble metal adatoms (Pd, Pt, Cu, Ag and Au) on a MoS<sub>2</sub> monolayer: A first-principles study," *Phys. Chem. Chem. Phys.*, vol. 19, no. 31, pp. 20713–20722, 2017.
- [46] Y. Wang, F. Kong, B. Zhu, S. Wang, S. Wu, and W. Huang, "Synthesis and characterization of Pd-doped α-Fe<sub>2</sub>O<sub>3</sub> H<sub>2</sub>S sensor with low power consumption," *Mater. Sci. Eng., B*, vol. 140, pp. 98–102, May 2007.
- [47] S. Peng, K. Cho, P. Qi, and H. Dai, "Ab initio study of CNT NO<sub>2</sub> gas sensor," *Chem. Phys. Lett.*, vol. 387, pp. 271–276, Apr. 2004.
- [48] Y.-H. Zhang *et al.*, "Improving gas sensing properties of graphene by introducing dopants and defects: A first-principles study," *Nanotechnology*, vol. 20, Apr. 2009. Art. no. 185504.



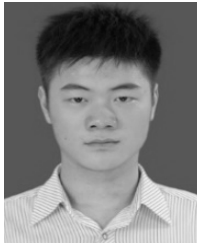
**ZHENWEI CHEN** was born in Putian, Fujian, China, in 1996. He received the bachelor's degree in electrical engineering and information technology from Sichuan University, Chengdu, China, in 2018. He is currently pursuing the master's degree with the School of Electric Engineering, Wuhan University, China. His research interests include the decomposition mechanism of insulating gas SF<sub>6</sub> and the fault diagnosis of high-voltage electrical insulation equipment.



**XIAOXING ZHANG** was born in Qianjiang, Hubei, China, in 1972. He received the bachelor's and master's degrees from the Hubei University of Technology, in 1993 and 1997, respectively, and the Ph.D. degree from Chongqing University, in 2006. His research interests include the online monitoring and fault diagnosis of high-voltage electrical insulation equipment, alternative gases of SF<sub>6</sub>, the decomposition mechanism of SF<sub>6</sub>, and the new nano-sensor.



**HAO XIONG's** research interests include the online monitoring and fault diagnosis of high-voltage electrical insulation equipment.



**DACHANG CHEN** was born in Wuhan, Hubei, China, in 1993. He received the bachelor's degree in electrical engineering from Wuhan University, Wuhan, in 2016, where he is currently pursuing the Ph.D. degree with the School of Electric Engineering. His research interests include the decomposition mechanism of insulating gas SF<sub>6</sub> and the new nano-sensor.



**HONGTU CHENG** was born in Puyang, Henan, China, in 1996. He is currently pursuing the master's degree with the School of Electrical and Automation, Wuhan University. His research interests include the online monitoring and fault diagnosis of power equipment.



**JU TANG** was born in Pengxi, Sichuan, China, in 1960. He received the B.Sc. degree from Xi'an Jiaotong University, Xi'an, China, in 1982, and the M.Sc. and Ph.D. degrees from Chongqing University, Chongqing, China, in 2000 and 2004, respectively. He is currently a Professor with the School of Electrical Engineering, Wuhan University, and also the Chief Scientist presiding over the National Basic Research Program of China (973 Program) (2009CB724506). His research interests include high-voltage equipment online monitoring, fault diagnosis, signal processing, simulation analysis, and pattern recognition.



**YUAN TIAN** was born in Hengyang, Hunan, China, in 1996. He received the bachelor's degree in electrical engineering from the Wuhan University of Technology, where he is currently pursuing the master's degree in electrical engineering.



**SONG XIAO** was born in Zhangjiakou, Hebei, China, in 1988. He received the B.S. and Ph.D. degrees in electrical engineering from Chongqing University, Chongqing, China, and the Ph.D. degree in plasma engineering from the Université de Toulouse, Toulouse, France. He is an Associate Professor with the School of Electric Engineering and Automation, Wuhan University. His research interests include partial discharge online monitoring and gas substituting SF<sub>6</sub>.

...